

Dual-Attention Residual Network for Automatic Diagnosis of COVID-19

Jun Shi¹, Huite Yi¹, Xiaoyu Hao¹, Hong An¹, and Wei Wei²

¹ University of Science and Technology of China

² Department of Radiology, The First Affiliated Hospital, Division of Life Sciences and Medicine, University of Science and Technology of China

Abstract. The ongoing global pandemic of Coronavirus Disease 2019 (COVID-19) has posed a serious threat to public health and the economy. Rapid and accurate diagnosis of COVID-19 is crucial to prevent the further spread of the disease and reduce its mortality. Chest computed tomography (CT) is an effective tool for the early diagnosis of lung diseases including pneumonia. However, detecting COVID-19 from CT is demanding and prone to human errors as some early-stage patients may have negative findings on images. In this study, we propose a novel residual network to automatically identify COVID-19 from other common pneumonia and normal people using CT images. Specifically, we employ the modified 3D ResNet18 as the backbone network, which is equipped with both channel-wise attention (CA) and depth-wise attention (DA) modules to further improve the diagnostic performance. Experimental results on the large open-source dataset show that our method can differentiate COVID-19 from the other two classes with 94.7% accuracy, 93.73% sensitivity, 98.28% specificity, 95.26% F1-score, and an area under the receiver operating characteristic curve (AUC) of 0.99, outperforming baseline methods. These results demonstrate that the proposed method could potentially assist the clinicians in performing a quick diagnosis to fight COVID-19.

Keywords: COVID-19 · Automatic Diagnosis · Residual Network.

1 Introduction

The Coronavirus Disease 2019 (COVID-19), caused by the severe acute respiratory symptom coronavirus 2 (SARS-CoV-2), is spreading rapidly across the world through extensive person-to-person transmission [4]. The World Health Organization (WHO) officially declared the COVID-19 a pandemic on 11 March 2020. As of 20 February 2021, the COVID-19 has infected more than 110 million people in more than 192 countries and territories and caused more than 2.45 million deaths [5]. Due to the persistent lack of clinically proven antiviral drugs and vaccines available for treatment, the COVID-19 pandemic has had a devastating impact on public health and the economy. It is of great importance to conduct early diagnosis of COVID-19, for preventing the further spread of the disease and delivering proper treatment regimen.

The real-time reverse transcription-polymerase chain reaction (RT-PCR) test is the golden standard for the diagnosis of COVID-19 infection [28]. However, the high false-negative rate [4] of RT-PCR may delay the diagnosis of potential cases. Moreover, RT-PCR testing is often time-consuming, and the clinicians suffer from the risk of infection. These factors underline the urgent need for alternative methods for rapid and accurate diagnosis of COVID-19.

Chest X-ray and computed tomography (CT) are two valuable tools for the early diagnosis of patients suspected of SARS-CoV-2 infection [13]. Compared with X-ray images, chest CT scans have higher sensitivity in diagnosing COVID-19 infection, and can provide more detailed information about the lesion, which is helpful for quantitative analysis [1]. Early investigations have observed typical radiographic features on chest CT images such as ground-glass opacities (GGO), multifocal patchy consolidation, and vascular dilation in the lesions [21, 19, 18, 2]. However, detecting COVID-19 from CT images is demanding and prone to human errors as some early-stage patients may have normal imaging features. Besides, the similar imaging findings between COVID-19 and other common pneumonia on the image make it difficult to differentiate.

Therefore, we propose a dual-attention residual network to automatically diagnose COVID-19 from other common pneumonia and normal people using CT images. In our method, the 3D variant of ResNet18 [8] is used as the backbone network, which takes a full 3D chest CT image as input. To improve the diagnostic performance, we employ two attention mechanisms: 1) channel-wise attention and 2) depth-wise attention, to refine the hidden features. The former is first proposed in [11], and we implement its 3D extension. In this study, we develop the latter, which can adaptively assign depth-level weights to each feature map during the training. We evaluate our method on the largest open-source CT image dataset, to the best of our knowledge. The experimental results show that the proposed method outperforms the baseline method and some existing methods. We further provide ablation studies and prove the effectiveness of the proposed depth-wise attention module in improving the classification accuracy and the interpretability of the model.

As a summary, we propose a dual-attention convolutional neural network (CNN) that may meet the urgent need for the automatic diagnosis of COVID-19 in clinical practice. Our work has three major contributions as follows:

- We develop a 3D network to realize automatic and accurate diagnosis of COVID-19 using CT images. Evaluated on a large open-source dataset, the proposed method can identify COVID-19 from other common pneumonia and the normal with 94.7% accuracy, 93.73% sensitivity, 98.28% specificity, 95.26% F1-score, and an area under the receiver operating characteristic curve (AUC) of 0.99.
- The depth-wise attention module we proposed can improve the classification performance and the interpretability of 3D ResNet with only a slight increase in computational complexity. Moreover, the module has good scalability and can be easily inserted into any 3D CNN-based method along with other attention mechanisms.

- Our method is end-to-end trainable and readily applicable to other clinical diagnostic problems, such as predicting pneumonia subtypes.

2 Related Work

Automatic Diagnosis of COVID-19: Recently, the successful application of artificial intelligence (AI) in medical image analysis [16] has promoted the development of radiological diagnosis technology. To combat the current pandemic, plenty of research efforts have been carried out over the past few months to design an AI system for the early diagnosis of COVID-19 via radiological imaging. Wang et al. [23] and Zhang et al. [24] employ CNNs to automatically identify COVID-19 infection from chest X-ray images and obtain promising results. However, it is still a challenging task due to the low contrast and the lack of significant features caused by the high overlapping of ribs and soft tissues.

Compared with a single X-ray image, a chest CT scan composed of hundreds of 2D slices can reflect more detailed radiographic features about the lesions, such as GGO and consolidation. To simplify the computation, several keyframe-based methods [18,7] are proposed to diagnose COVID-19 in CT images. Although these methods ignore the inter-slice information of CT images and highly rely on the accurate detection of abnormal slices. Besides, [25,20,15] propose the segmentation-based approaches that can generate more specific lesion information, such as the number and volume of lesions, which is valuable for the quantitative analysis in COVID-19 diagnosis. However, obtaining large amounts of annotated CT data is the primary challenge of these methods. We thus develop a novel 3D network to identify COVID-19 in an end-to-end fashion, which only takes a full chest CT image as input and can achieve competitive classification performance.

Attention Mechanism: Attention mechanism is an effective way to improve network performance by enhancing the learned features. Hu et al. [11] propose the channel-wise attention (CA) to refine the hidden features in the channel dimension during training, which can make the network more focused on the important regions. The effectiveness of the CA module has been proved in many applications [3,6,26]. Inspired by this, we develop a novel attention mechanism called depth-wise attention (DA) to weight the depth-level features to further improve the representation ability of the 3D network.

Class Activation Mapping: To explore the interpretability of CNN-based methods, some visualization techniques have been proposed such as class activation mapping (CAM) [27] and Grad-CAM [22], which can reveal the discriminative regions affecting the network prediction. In this study, we apply CAM to analyze the differences in decision-making factors among different networks.

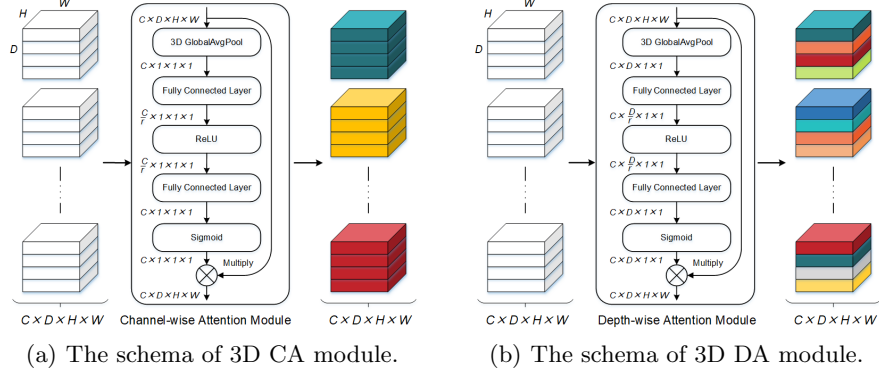


Fig. 1. Illustration of the channel-wise attention (CA) and the proposed depth-wise attention (DA) modules in our method. D , H , W , and C represent the depth, height, width, and input channels of the feature map, and r refers to the reduction ratio.

3 Method

3.1 Backbone Network

Considering the computation complexity and GPU memory capacity, we use the 3D ResNet18 [8] as the backbone network. Then, we replace the original residual block with a new one, which consists of two consecutive 3D convolutional layers followed by two attention mechanisms: 1) channel-wise attention and 2) depth-wise attention. Besides, we set the stride of the depth dimension as 1 in the first convolutional layer and reduce one downsampling operation. In this way, the input CT image is downsampled by a factor of 8 in the depth dimension and a factor of 16 in the other two dimensions. The higher-resolution feature maps retain more contextual information, which is conducive to visual analysis.

3.2 Depth-wise Attention Module

A CT image is usually composed of hundreds of 2D slices stacked in sequence. These slices have high spatial continuity and content relevance, constituting the complete contextual information of the lungs. Moreover, we observe that the lesions of various sizes appear randomly in the lungs, resulting in only a portion of the slices containing visible disease characterizations. The spatial correlations of different dimensions and the inter-slice information will be entangled by a 3D convolution operator when using 3D CNN to directly classify CT images. Hu et al. [11] propose the channel-wise attention (CA) module to enhance channel independence and thereby improve the performance of the networks. Inspired by this, we design a novel mechanism called depth-wise attention (DA) module for 3D CNN to weight the depth-level features, which can make the network more sensitive to the important regions of the images.

In the DA module, the spatial information is aggregated first along the depth axis by global average pooling (GAP) layer, as shown in Fig. 1. Considering the input feature map $\mathbf{F}_{\text{in}} \in \mathbb{R}^{C \times D \times H \times W}$ and $\mathbf{F}_{\text{in}} = [\mathbf{f}^{1,1}, \mathbf{f}^{1,2}, \dots, \mathbf{f}^{i,j}, \dots, \mathbf{f}^{C,D}]$, where C , D , H , and W are the input channels, depth, height, and width, respectively, and $\mathbf{f}^{i,j} \in \mathbb{R}^{H \times W}$. The output of the GAP represented by $\mathbf{Z} \in \mathbb{R}^{C \times D \times 1 \times 1}$ with its element

$$z^{i,j} = \frac{1}{H \times W} \sum_{h=1}^H \sum_{w=1}^W \mathbf{f}^{i,j}(h, w). \quad (1)$$

Then, a gating mechanism is designed to learn non-linear and non-mutually-exclusive relationships in the depth dimension. The gating mechanism is parameterized by two fully-connected layers and two non-linearity activation functions. The output is $\hat{\mathbf{Z}} = \sigma(\mathbf{W}_2(\xi(\mathbf{W}_1\mathbf{Z})))$, with \mathbf{W}_1 , \mathbf{W}_2 being the weights of two fully-connected layers, the ReLU function $\xi(\cdot)$ and the sigmoid function $\sigma(\cdot)$. The resultant tensor is used to refine \mathbf{F}_{in} to

$$\mathbf{F}_{\text{out}} = [\hat{z}^{1,1}\mathbf{f}^{1,1}, \hat{z}^{1,2}\mathbf{f}^{1,2}, \dots, \hat{z}^{i,j}\mathbf{f}^{i,j}, \dots, \hat{z}^{C,D}\mathbf{f}^{C,D}]. \quad (2)$$

The DA module recalibrates the depth-level features by adaptively assigning weights, which can make the network more focused on the important regions distributed sparsely along the depth dimension. By combining DA and CA modules, we construct the dual-attention residual module for our network.

4 Experiments

4.1 Dataset and Metrics

Table 1. The statistics and division of our dataset. The dataset is divided into the training and test cohorts.

#Scan	COVID-19	Common pneumonia	Normal controls	In total
Training cohort	1320	1328	952	3600
Test cohort	169	177	126	472
In total	1489	1505	1078	4072

In this study, we collect 4,072 full chest CT scans from the website¹ of China Consortium of Chest CT Image Investigation (CC-CCII). The CT dataset contains 1,489 CT scans of COVID-19 patients, 1,505 CT scans of common pneumonia patients, and 1,078 CT scans of normal controls. As shown in Table 1, 3600 scans (1320 COVID-19 cases, 1328 common pneumonia cases, and 952 normal controls) and 472 scans (169 COVID-19 cases, 177 common pneumonia cases,

¹ <http://ncov-ai.big.ac.cn/download?lang=en>

and 126 normal controls) are used for training and independent testing, respectively. Besides, the training set is randomly divided into five folds on patient level for cross-validation.

In the test stage, we apply several classification metrics including the area under the receiver operating characteristic curve (AUC), accuracy, sensitivity, specificity, and F1-score, to evaluate the performance of different networks.

4.2 Implementation Details

Pytorch is adopted to implement our proposed method. For training the network, we use Adam optimizer [14] to minimize the cross-entropy loss with an initial learning rate of 10^{-3} . The convolutional layer weights are initialized by the Kaiming Normalization [9] and the biases are set to 0. Besides, we apply the cosine annealing strategy [17] to control the change of the learning rate during training. Given the limitation of GPU memory, the batch size is set to 4 and the size of all scans is fixed to $64 \times 224 \times 224$ by under-sampling or up-sampling. To alleviate the overfitting problem, we conduct online data augmentation including random flipping, rotation, translation, and scaling. The codes used in the experiments will be made publicly available.

4.3 Comparison of Different Methods

Table 2. The performance comparison between different methods of identifying COVID-19 on the different test sets (all from CC-CCII). For the results on the independent test set of the baseline model (ResNet18) and our method, we show the mean \pm std (standard deviation) scores of five trained models of each training-validation fold. Larger values indicate better performance, and - denotes no relevant data.

Method	ResNet18	[25]	[12]	[10]	Ours
Test cohort(#Scan)	472	389	3784	798	472
AUC	0.9890 \pm 0.0045	0.9797	0.9212	0.9400	0.9900\pm0.0016
Accuracy	0.9250 \pm 0.0219	0.9249	-	0.8863	0.9470\pm0.0054
Sensitivity	0.9124 \pm 0.0597	0.9493	0.7799	0.8609	0.9373\pm0.0090
Specificity	0.9881 \pm 0.0098	0.9113	0.9355	0.9435	0.9828\pm0.0137
F1-score	0.9429 \pm 0.0288	-	-	0.8814	0.9526\pm0.0072

We use 3D ResNet18 as the baseline model and compare the performance of our method with several existing methods. The test cohorts of different sizes used by these methods all come from CC-CCII. In particular, [25] and [12] are segmentation-based methods, which rely on accurate segmentation of the lesions. [10] provides a benchmark for COVID-19 detection using deep learning models. The benchmark tests multiple models and we choose the best performing one for

comparison. As shown in Table 2, we can see that the proposed method achieves the best performance with 94.7% accuracy, 93.73% sensitivity, 98.28% specificity, 95.26% F1-score, and AUC of 0.99. These results prove the superiority of our method in identifying COVID-19 from other common pneumonia and the normal. Besides, the comparison between ResNet18 and our method, demonstrates that our modification has a practical effect on improving performance.

4.4 Ablation Studies of Different Modules

Table 3. For COVID-19 versus the other two classes (common pneumonia and the normal controls), we compare the results of the ablation studies on DA module and CA module ($\sqrt{\times}$ denotes with/without). Five folds cross-validation is used.

Network	ResNet18	CA-ResNet18	DA-ResNet18	Ours
DA	\times	\times	\sqrt	\sqrt
CA	\times	\sqrt	\times	\sqrt
AUC	0.9890 ± 0.0045	0.9930 ± 0.0014	0.9892 ± 0.0027	0.9900 ± 0.0016
Accuracy	0.9250 ± 0.0219	0.9385 ± 0.0113	0.9407 ± 0.0095	0.9470 ± 0.0054
Sensitivity	0.9124 ± 0.0597	0.9373 ± 0.0123	0.9243 ± 0.0164	0.9373 ± 0.0090
Specificity	0.9881 ± 0.0098	0.9908 ± 0.0118	0.9901 ± 0.0040	0.9828 ± 0.0137
F1-score	0.9429 ± 0.0288	0.9648 ± 0.0126	0.9518 ± 0.0074	0.9526 ± 0.0072
Parameters	33.15M	33.24M	35.24M	35.15M

To validate the effectiveness of the proposed attention module, we conduct ablation studies on CA and DA modules. Table 3 quantitatively compare the performance of different networks on the same test set. For COVID-19 versus the other two classes (common pneumonia and the normal controls), our method equipped with both CA and DA modules achieves the highest accuracy and sensitivity, while the parameter is only increased by $\sim 6.3\%$ compared with ResNet18. The results of the ablation experiments prove the effectiveness of the CA and DA modules in improving the classification performance of ResNet18. Especially, the dual-attention module can achieve a higher performance improvement than a single CA or DA module in this task.

4.5 Visualization and Analysis

To explore the interpretability of the proposed method, we employ CAM [27] to visualize the discriminative regions of different networks in diagnosing COVID-19. Fig. 2 shows the visualization results on three COVID-19 cases with different degrees (mild, moderate, and severe) of infection, highlighting the regions that the network focuses on when making decisions. We can see that the outputs of the networks with CA or DA module added can roughly indicate the lesion

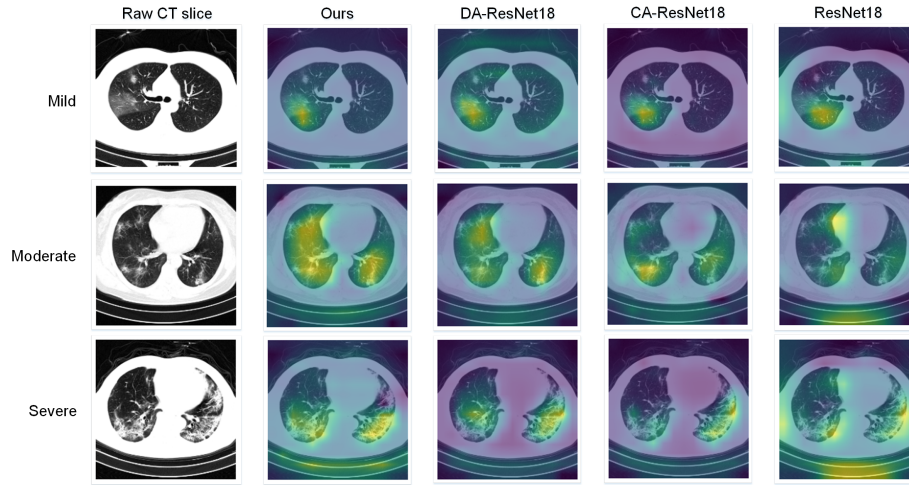


Fig. 2. Visualization results of different methods on three COVID-19 cases with different degrees of infection are shown from top to down, respectively. The discriminative regions of different networks are highlighted.

location. In contrast, only ResNet18 is less sensitive to lesions, and may even be disturbed by the information outside the lung area. The above results demonstrate that DA and CA modules can enhance the learned features to ensure that the decisions made by the network depend mainly on the infection regions, rather than the irrelevant parts of the images. More importantly, the results show that our method has better interpretability and reliability in diagnosing COVID-19, which is the basis for its application in clinical practice.

5 Conclusion

In this work, we propose a dual-attention residual network that can realize the automatic and accurate diagnosis of COVID-19 using CT images. In our method, we develop a depth-wise attention module to refine the hidden depth-level features by adaptively assigning weights during training. This module can improve the performance and interpretability of 3D ResNet, while only slightly increasing the computational complexity. We evaluate our method on the largest public CT dataset (to the best of our knowledge). The experimental results show that the proposed method outperforms the baseline method and some existing methods. In future work, we will use more data to test the generalization ability of our method. Moreover, we are interested in extending the proposed approach to other clinical diagnostic problems, such as predicting pneumonia subtypes.

References

1. Ai, T., Yang, Z., Hou, H., et al.: Correlation of Chest CT and RT-PCR Testing for Coronavirus Disease 2019 (COVID-19) in China: A Report of 1014 Cases. *Radiology* **296**(2), E32–E40 (2020)
2. Butt, C., Gill, J., Chun, D., Babu, B.A.: Deep learning system to screen coronavirus disease 2019 pneumonia. *Applied Intelligence* (2020)
3. Cao, Y., Xu, J., Lin, S., Wei, F., Hu, H.: GCNet: Non-local networks meet squeeze-excitation networks and beyond. *Proceedings - 2019 International Conference on Computer Vision Workshop, ICCVW 2019* pp. 1971–1980 (2019)
4. Chan, J.F.W., Yuan, S., Kok, K.H., et al.: A familial cluster of pneumonia associated with the 2019 novel coronavirus indicating person-to-person transmission: a study of a family cluster. *The Lancet* **395**(10223), 514–523 (Feb 2020)
5. Dong, E., Du, H., Gardner, L.: An interactive web-based dashboard to track covid-19 in real time. *The Lancet Infectious Diseases* **20**(5), 533–534 (May 2020)
6. Gao, S., Cheng, M.M., Zhao, K., Zhang, X.Y., Yang, M.H., Torr, P.H.: Res2Net: A New Multi-scale Backbone Architecture. *IEEE Transactions on Pattern Analysis and Machine Intelligence* **8828**(c), 1–1 (2019)
7. Hasan, A.M., Al-Jawad, M.M., et al.: Classification of Covid-19 coronavirus, pneumonia and healthy lungs in CT scans using Q-deformed entropy and deep learning features. *Entropy* **22**(5) (2020)
8. He, K., Zhang, X., Ren, S., Sun, J.: Deep residual learning for image recognition. *CoRR* **abs/1512.03385** (2015)
9. He, K., Zhang, X., Ren, S., Sun, J.: Delving deep into rectifiers: Surpassing human-level performance on imagenet classification. *arXiv preprint arXiv: 1502.01852* (2015)
10. He, X., Wang, S., Shi, S., Chu, X., et al.: Benchmarking deep learning models and automated model design for COVID-19 detection with chest CT scans. *medRxiv* pp. 1–13 (2020). <https://doi.org/10.1101/2020.06.08.20125963>
11. Hu, J., Shen, L., Sun, G.: Squeeze-and-excitation networks. *CoRR* **abs/1709.01507** (2017)
12. Jin, C., Chen, W., Cao, Y., et al. Jie, Shi, H., Feng, J.: Development and evaluation of an artificial intelligence system for COVID-19 diagnosis. *Nature Communications* **11**(1) (2020). <https://doi.org/10.1038/s41467-020-18685-1>
13. Kadry, S., Rajinikanth, V., Rho, S., Raja, N.S.M., Rao, V.S., Thanaraj, K.P.: Development of a Machine-Learning System to Classify Lung CT Scan Images into Normal/COVID-19 Class. *arXiv preprint arXiv: 2004.13122* (2020)
14. Kingma, D.P., Ba, J.: Adam: A method for stochastic optimization. *arXiv preprint arXiv: 1412.6980* (2014)
15. Li, L., Qin, L., Xu, Z., et al.: Using artificial intelligence to detect covid-19 and community-acquired pneumonia based on pulmonary ct: Evaluation of the diagnostic accuracy. *Radiology* **296**(2), E65–E71 (Aug 2020)
16. Litjens, G., Kooi, T., Bejnordi, B.E., et al.: A survey on deep learning in medical image analysis. *Medical Image Analysis* **42**, 60 – 88 (2017)
17. Loshchilov, I., Hutter, F.: SGDR: stochastic gradient descent with restarts. *CoRR* **abs/1608.03983** (2016)
18. Mei, X., Lee, H.C., et al.: Artificial intelligence-enabled rapid diagnosis of patients with COVID-19. *Nature Medicine* **26**(8), 1224–1228 (2020)
19. Nishiura, H., Jung, S.M., Linton, N.M., Kinoshita, R., Yang, Y., et al.: The extent of transmission of novel coronavirus in wuhan, china, 2020. *Journal of clinical medicine* **9**(2), 330 (Jan 2020)

20. Ouyang, X., Huo, J., Xia, L., et al.: Dual-Sampling Attention Network for Diagnosis of COVID-19 from Community Acquired Pneumonia. *IEEE Transactions on Medical Imaging* **39**(8), 2595–2605 (2020)
21. Phelan, A.L., Katz, R., Gostin, L.O.: The Novel Coronavirus Originating in Wuhan, China: Challenges for Global Health Governance. *JAMA* **323**(8), 709–710 (02 2020)
22. Selvaraju, R.R., Cogswell, M., Das, A., Vedantam, R., Parikh, D., Batra, D.: Grad-CAM: Visual Explanations from Deep Networks via Gradient-Based Localization. *International Journal of Computer Vision* **128**(2), 336–359 (2020)
23. Wang, L., Wong, A.: COVID-Net: A Tailored Deep Convolutional Neural Network Design for Detection of COVID-19 Cases from Chest X-Ray Images. *arXiv preprint arXiv: 2003.09871* (2020)
24. Zhang, J., Xie, Y., Liao, Z., Pang, G., Verjans, J., Li, W., Sun, Z., He, J., Li, Y., Shen, C., Xia, Y.: Viral Pneumonia Screening on Chest X-ray Images Using Confidence-Aware Anomaly Detection. *arXiv preprint arXiv: 2003.11988* (2020)
25. Zhang, K., Liu, X., Shen, J., et al., He, J., et al.: Clinically applicable ai system for accurate diagnosis, quantitative measurements, and prognosis of covid-19 pneumonia using computed tomography. *Cell* **181**(6), 1423 – 1433.e11 (2020)
26. Zhao, Q., Sheng, T., Wang, Y., Tang, Z., Chen, Y., Cai, L., Ling, H.: M2Det: A Single-Shot Object Detector Based on Multi-Level Feature Pyramid Network. *Proceedings of the AAAI Conference on Artificial Intelligence* **33**, 9259–9266 (2019)
27. Zhou, B., Khosla, A., Lapedriza, A., Oliva, A., Torralba, A.: Learning deep features for discriminative localization. In: *2016 IEEE Conference on Computer Vision and Pattern Recognition (CVPR)*. pp. 2921–2929 (2016)
28. Zu, Z.Y., Di Jiang, M., Xu, P.P., Chen, W., Ni, Q.Q., Lu, G.M., Zhang, L.J.: Coronavirus Disease 2019 (COVID-19): A Perspective from China. *Radiology* **296**(2), E15–E25 (2020)